Adaptive Hazard Zone Model for Improved Safety in Highway Work Zones

Ayenew Yihune Demeke[1], Moein Younesi Heravi[1], Israt Sharmin Dola[2], Inbae Jeong[2], and Youjin Jang[1]

[1]Dept. of Civil, Construction and Environmental Engineering, North Dakota State University, Fargo, ND, USA
[2]Dept. of Mechanical Engineering, North Dakota State University, Fargo, ND, USA
ayenew.demeke@ndsu.edu, moein.younesiheravi@ndsu.edu, israt.dola@ndsu.edu, inbae.jeong@ndsu.edu, y.jang@ndsu.edu

Abstract

Highway work zones present hazardous conditions where worker safety is at constant risk due to interactions with construction equipment. In such environments, accurately defining hazard zones around equipment is vital for timely detection and prevention of incidents. Traditional static hazard zone models, often relying on simple geometric shapes, fall short as they cannot adapt to changes in equipment speed and movement, leading to either inadequate safety coverage or frequent false alarms. This study proposes a dynamic hazard zone model that leverages a probabilistic approach based on bivariate Gaussian distribution to generate adaptive and realistic hazard zones. Real-time data from GPS and inertial measurement unit (IMU) sensors enable the model to adjust hazard zone dimensions dynamically in response to equipment behavior, improving both accuracy and responsiveness. Simulations conducted in Webots software demonstrated that the proposed model achieved 93% accuracy in hazard detection, significantly outperforming the 60% accuracy of static circular zones tested in the same environment. The findings underscore the potential of dynamic hazard zone modeling to enhance safety in highway work zones, providing a practical and effective approach for reducing risks.

Keywords –

Highway work zones, construction safety, probabilistic modeling, real-time tracking, dynamic hazard zones

1 Introduction

Highway work zones are inherently complex and hazardous environments where the safety of construction workers and motorists is constantly challenged by active construction and traffic flows. The increased number of accidents and fatalities associated with these zones has led researchers and practitioners to focus on developing more effective safety measures [1], [2]. Accidents in these areas can result from a variety of causes, including but not limited to vehicular collisions, worker-equipment interactions, and improper management of traffic flow [3]. A significant number of these accidents happen due to worker-equipment interactions, making the prevention of near-miss incidents and collisions a critical issue [4].

Effectively mapping the hazard zone around equipment plays a pivotal role in this context, serving as a crucial mechanism for incident detection [5], [6]. Traditional approaches to hazard zone mapping typically employ static models, which use simple geometric shapes, such as circles, to define areas of danger around construction equipment [7]. These models could, however, fall short in adequately providing the necessary protection due to two main reasons. First, these hazard zones have fixed sizes and provide the same hazard area, even when the equipment moves at different speeds [8]. This would lead to either an insufficient zone that could not timely detect hazards for equipment moving at a higher speed, or too large zone, which would lead to unnecessary alarms for equipment moving at a low speed or a stationary piece of equipment [9], [10]. The second reason is related to the shape of the hazard zone. The use of simple shapes like circles will lead to the marking of relatively safer areas, such as the sides of a moving vehicle, as hazardous, which could lead to false alarms [11], [12]. These issues are especially relevant in congested areas such as highway work zones where workers on foot and equipment work side by side in a relatively small area [13]. In such situations, if the hazard zones are not carefully designed to efficiently detect true hazardous situations and avoid any false alarm scenarios, it will lead to either insufficient protection for workers or repetitive false alarms, which could result in work disruption and desensitization [8], [14].

To address these problems, this study proposes an adaptive hazard zone model that dynamically adjusts the hazard boundaries in real-time based on equipment movement. The proposed model addresses the existing issues by creating a dynamic and more realistic hazard zone around the equipment, effectively mapping the real hazardous areas and avoiding safer areas. The study proposes a rigorous probabilistic approach to developing a mathematical hazard zone model that relies on equipment movement parameters to produce a hazard map with varying levels of safety around the equipment. Real time tracking of equipment movement is achieved by utilizing GPS and inertial measurement unit (IMU) sensors. The proposed model is validated in a simulated environment in Webots software, where several scenarios of realistic interactions between workers and construction equipment are evaluated.

2 Literature Review

Properly modelling hazard zones around construction equipment is essential for preventing near-miss and collision incidents between equipment and workers on foot. These zones must effectively detect and alert potential incidents, allowing both workers and equipment operators sufficient time to react safely. Additionally, the zones should be precise enough to avoid unnecessary alarms that could disrupt work or desensitize workers to genuine hazards. Various hazard zoning approaches exist in practice and in literature, each with its own advantages and limitations. The following sections discuss some of these methods.

2.1 Hazard Zone Models

Hazard zone modelling in construction and industrial environments traditionally relies on static models with fixed sizes, and typically utilizes simple geometric shapes to demarcate areas of danger around equipment. These static hazard zones have predefined danger areas around equipment that do not change shape or size in response to the equipment's real-time movement. Because static zones remain constant regardless of vehicle speed or direction, they can either overestimate or underestimate the true hazardous area in different scenarios.

Among the various static hazard zone approaches, the use of circular hazard zones is common in both practice and literature, with variations in how the circle's size and the number of hazard levels are determined. Wang & Razavi [6] proposed circular hazard and warning zones around a construction equipment. The warning zone represents the area where a warning should be issued when a worker breaches it while the hazard zone represents the actual dangerous area. Although the formulation in the study considered the speed and deceleration of the equipment for determining the braking distance, only typical values for a specific equipment were finally used to determine the dimensions of the hazard zone. Similarly, circular and rectangular hazard zones were explored in studies by Teizer et al. [7] and Luo et al. [15]. Jo et al. [14] also utilized circular hazard zones to represent hazardous areas around an excavator.

In an attempt to make circular zones more representative, Teizer & Cheng [11] proposed a hazard zone that considers only part of a circle, in the direction of the equipment's movement. The proposed hazard zone is also dynamic, adjusting its size based on equipment speed. Although the proposed hazard zone worked generally well, it was pointed out that there were missed hazards and false alarms during the experiment. A study by Shen et al. [5] proposed a standard procedure to come up with hazard zones with different shapes and sizes specific to the type and size of equipment. The procedure also uses typical equipment speed and deceleration values to determine the size of the hazard zone.

Although the studies mentioned above tried to consider several parameters to develop effective hazard zones, there is still a gap in providing a hazard zone model which both has a realistic representation of the actual hazardous area and adapts its size based on real-time equipment movement information. Park et al. [8] affirms this by stating that previous research has insufficiently investigated the variations in proximity sensing caused by different settings such as equipment types and approaching speeds. The study further recommends future research to focus on defining dynamic hazard zones based on factors such as approaching speeds.

Another key aspect to consider is the level of hazard that these zones represent. Many proposed methods provide a single hazard zone, which defines whether a worker is either inside or outside a hazardous area [11], [14]. In contrast, some methods suggest a multi-level hazard zoning approach, which establishes warning and alert areas to offer an additional layer of safety by distinguishing between moderate and critical risk levels [7]. Teizer [16] used three levels of hazard, corresponding to "warn," "slow," and "stop", during field experiment of a proposed magnetic field-based proximity detection and alert system.

Overall, previous literature highlights the need for a hazard zoning methodology where the hazard zone adjusts its size and shape in real-time based on equipment behavior. Such a model would significantly enhance the accuracy of detecting and preventing near-miss incidents. In addition, provision of multiple zones corresponding to varying levels of hazard would be beneficial to give early warnings before a more dangerous situation happens.

Probabilistic approaches are increasingly gaining traction in hazard zoning to improve risk estimation and adaptability in construction and industrial settings, though there is limited research in applying them for modeling hazard zones around a vehicle. Studies have explored probabilistic risk assessments in construction and industrial environments to enhance safety performance. Park et al. [17] developed a sensor-based safety risk model that quantifies hazard exposure using probabilistic evaluation methods. Zhang et al. [18] applied stochastic processes to model safety risk in construction, demonstrating how probability-driven methods can improve accident prediction. Similarly, Abdrakhmanova et al. [19] proposed a probabilistic hazard analysis framework for industrial operations, incorporating dynamic exposure zones. While these studies demonstrate the benefits of probabilistic approaches in various domains, their application to highway work zones and to model vehicle hazard zones remains largely unexplored.

2.2 Recent Advances in Real-Time Location Systems

Implementing an adaptive hazard zone requires real-time tracking of equipment speed and acceleration. Recent technological advances, particularly in IoT-based applications, have significantly improved the feasibility of real-time data collection in construction environments. Real-time location systems (RTLS) are now frequently deployed in various industries to track the positions of workers, vehicles, and equipment. In construction, these systems could offer substantial benefits in various areas including safety improvements by monitoring proximity and movement in hazardous areas [20], [21].

RTLS employs a range of technologies, including GPS, IMU, radio frequency identification (RFID), Ultra-Wideband (UWB), and Bluetooth, to achieve precise location tracking. These technologies allow for real-time monitoring of assets and workers, enhancing situational awareness in complex, dynamic environments like highway work zones [22], [23], [24]. The use of these sensors allows accurate real-time tracking, which could be crucial for creating adaptive safety zones that adjust based on equipment speed and worker proximity [25].

With real-time data from IoT-based systems, it is now feasible to create hazard zones that expand or contract in response to movement, ensuring more precise safety measures than traditional static models. Such systems have been shown to improve both safety and efficiency on sites where real-time tracking of workers and equipment is crucial, as noted by Teizer et al. [26] in their study on LoRaWAN applications for tracking in construction environments.

3 Methodology

The aim of this study is developing an adaptive hazard zone model for construction equipment with a more realistic hazard zone area using a probabilistic approach. The use of probabilistic method enabled mapping the area around the equipment as a continuous zone with varying levels of hazard risk. The methodology used in this study generally included two main steps: theoretical derivation of a hazard zone model and testing in a simulated environment. In the theoretical derivation, the issues discussed in the previous sections, namely, having a more realistic hazard zone geometry, making it adaptive to equipment speed and direction, and providing zones for varying hazard levels, were addressed by utilizing a probabilistic approach.

3.1 Hazard Zone Model Development

A probabilistic approach with a bivariate Gaussian distribution is used to derive a hazard zone model. This resulted in a 3D graph that not only provides more representative elliptical hazard zones with adaptive major and minor axes but also allows to determine the probability of hazard at any location from the position of the equipment. A series of elliptical projections with the required probability of hazard can be extracted from the graph to represent varying levels of safety around the equipment (Figure 1). The colors of the ellipses in the figure represent an increasing level of hazard in moving towards the equipment, with the red color representing the highest level of hazard and the green one representing the lowest.

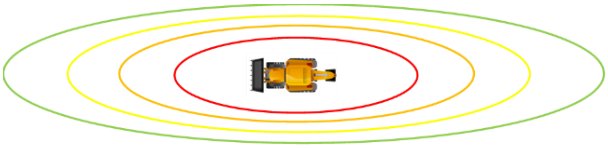

Figure 1. Elliptical projections from the proposed 2D Gaussian graph representing different hazard levels

The equation for a bivariate Gaussian distribution is given in Eq. 1, for independent variables x and y. The expression mainly involves four parameters: the mean and standard deviation values in both directions. The center of the distribution is taken to be at the center of the equipment and in line with this the mean values in both directions are taken to be zero. The standard deviation σ_x controls the spread along the x-axis while σ_y controls the spread along the y-axis. These standard deviations are made to be functions of the equipment's speed.

$$f(x,y) = \frac{1}{2\pi\sigma_x\sigma_y} \exp\left(-\frac{1}{2}\left[\frac{(x-\mu_x)^2}{{\sigma_x}^2} + \frac{(y-\mu_y)^2}{{\sigma_y}^2}\right]\right) \quad (1)$$

This study employs a six-step procedure to draw hazard zones around various construction equipment, as suggested by Shen et al. [5]. These procedures are generally followed to determine the necessary variables used in the derivation, except for the last step, where a different formulation is used in this study.

1. **Equipment Footprint:** This parameter represents the overall dimensions of the equipment, which depend on the type of equipment. For this derivation, the length (L) and width (W) of the equipment are considered as variables, allowing for flexibility in applying the model to different types of equipment.
2. **Initial Safety Boundary:** The initial safety boundary, represented by S in this study, defines the hazard zone when the equipment is stationary and is also treated as a variable in this derivation.
3. **Equipment Function:** This step involves determining the required safety distance based on the function and type of movement involved in the equipment. For example, the hazard zone of an excavator will have a circular shape with a radius governed by the size of the rotating arm. This study focused on moving equipment such as wheel loaders and dump trucks, with a hazard zone governed by the speed of the equipment. Choosing the type and function of the equipment forms the basis for computing parameters that influence the size of the hazard zone such as the distance required for the equipment to stop once a hazard is perceived by the operator, which is addressed in steps 4 and 5.
4. **Operator Reaction Distance (D_R):** The reaction distance is the distance covered by the equipment between the moment the operator perceives the hazard and takes measure (Eq. 2). It is computed as:
$$D_R = vt \quad (2)$$
Where v is the speed of the equipment in m/s, and t is the reaction time. The reaction time t is recommended to be 2.5 seconds [6], [27]. Thus, the equation simplifies to:
$$D_R = 2.5v \quad (3)$$
5. **Braking Distance (D_B):** The braking distance is the distance the equipment travels between the moment the operator takes action, and the equipment comes to a full stop, as given in Eq. 4 [5].
$$D_B = \frac{v^2}{2a} \quad (4)$$
Where v is the speed of the equipment in m/s, and a is the deceleration of the equipment in m/s². The deceleration could be different depending on the type of equipment. For example, a deceleration value of 1.9 m/s² is taken in Wang & Razavi [6] for forklift. In this study, it is considered as a variable, so that appropriate value could be assigned for a specific type of equipment later.
6. **Determine Hazard Zone:** The final step involves determining the resulting hazard zone based on steps 1 through 5. As mentioned above, the hazard zone is taken to be elliptical in shape, following the projection of a bivariate Gaussian distribution with the major axis representing the direction of movement of the equipment. The lengths of the major and minor axis of the ellipse are computed based on the values in the previous steps as described in Eq. 5 to Eq. 7.

Major axis:
$$Major\ axis = L + 2S + 2D_R + 2D_B \quad (5)$$
Where L is the length of the equipment, S is the initial safety boundary, D_R is the reaction distance, and D_B is the breaking distance. Therefore,
Major axis:
$$Major\ axis = L + 2S + 5v + \frac{v^2}{a} \quad (6)$$
Minor axis:
$$Minor\ axis = W + 2S \quad (7)$$

To determine σx and σy, these values are equated with the equation of an ellipse for a typical projection of the proposed bivariate Gaussian probabilistic plot, taking the hazard zone to be the ellipse with a 70% probability of hazard. This could be done for different probability values to derive different safety boundaries for different levels of hazard.

For a bivariate Gaussian distribution, the equation for an ellipse representing a specific probability contour is given in Eq. 8.
$$\left(\frac{x-\mu_x}{\sigma_x}\right)^2 + \left(\frac{y-\mu_y}{\sigma_y}\right)^2 = k \quad (8)$$
Where k is a constant corresponding to a specific confidence level. For a 70% confidence level, the value is obtained from the chi-squared distribution table to be approximately 0.713.

For a bivariate Gaussian distribution, the major and minor axes of the ellipse can be expressed in terms of the standard deviations as in Eq. 9 and Eq. 10.
Major axis:
$$Major\ axis = 2\sigma_x\sqrt{k} \quad (9)$$
Minor axis:
$$Minor\ axis = 2\sigma_y\sqrt{k} \quad (10)$$

Equating Eq. (9) and (10) with the corresponding expressions obtained earlier for the major and minor axes will result in an equation for the standard deviations in terms of equipment parameters.
Major axis:
$$2\sigma_x\sqrt{k} = L + 2S + 5v + \frac{v^2}{a} \quad (11)$$
$$\sigma_x = C_1L + C_2S + C_3v + C_4\frac{v^2}{a} \quad (12)$$
Minor axis:
$$2\sigma_x\sqrt{k} = W + 2S \quad (13)$$

$$\sigma_y = C_5 W + C_6 S \quad (14)$$

Where $C_1 = 0.592$, $C_2 = C_6 = 1.183$, $C_3 = 2.959$, and $C_4 = C_5 = 0.592$ are the coefficients.

The final expressions for the standard deviations show that the size of the hazard zone along the major axis of the ellipse depends on the real-time speed and the deceleration rate of the equipment, while the size in the cross-sectional direction remains constant. If the equipment turns, the major axis will change direction accordingly keeping the hazard zone aligned with the equipment's direction of movement.

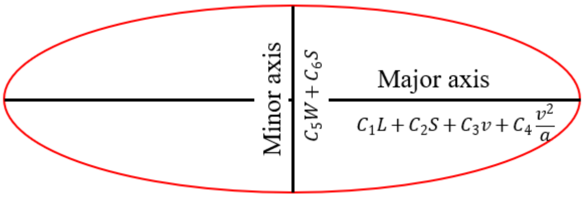

Figure 2. Hazard zone dimensions

In practical applications, real-time GPS/IMU sensor data will be used to continuously track the equipment's location, ensuring that the center of the hazard zone remains properly aligned with its current position. Additionally, these sensors will provide velocity and acceleration measurements, enabling the dynamic adjustment of the hazard zone size using Equations (12) and (14). To enhance accuracy and mitigate sensor noise, efficient sensor fusion techniques should be employed to effectively integrate GPS and IMU readings.

3.2 Simulation Setup

The primary objective of the simulation was to evaluate the effectiveness of the proposed hazard zone model in correctly detecting near-miss incidents at the right time. The simulation was conducted in Webots R2023b, an open-source desktop application from Cyberbotics, primarily used for robot simulations. The software was chosen for its strengths in effectively creating realistic road and traffic environments [28].

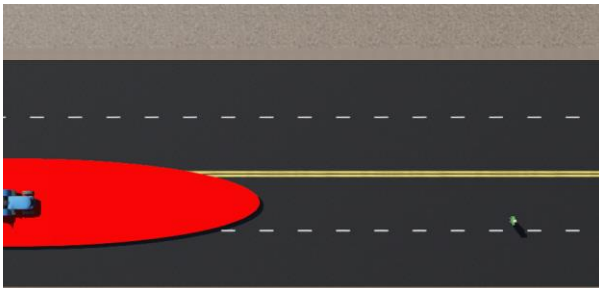

Figure 3. Simulation setup in Webots

The strategy involved driving equipment, equipped with GPS and IMU sensors, towards a worker positioned in front of it. A hazard zone was generated around the equipment, and when the worker entered the hazardous area, the equipment began decelerating, mimicking an operator's response upon being alerted (Figure 3). The equipment continued at its current speed for 2.5 seconds to simulate operator reaction time, then decelerated at the typical rate for the equipment in the simulation environment. The stopping position was evaluated to determine whether the hazard zone provided sufficient time for the equipment to stop. The simulation was conducted using the proposed dynamic hazard zone, and a static circular hazard zone for comparison (Figure 4).

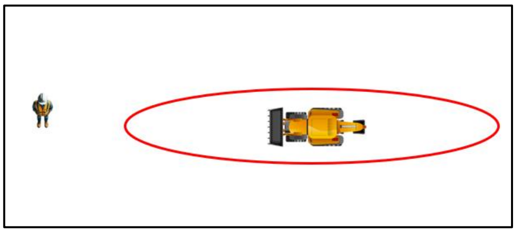

(a)

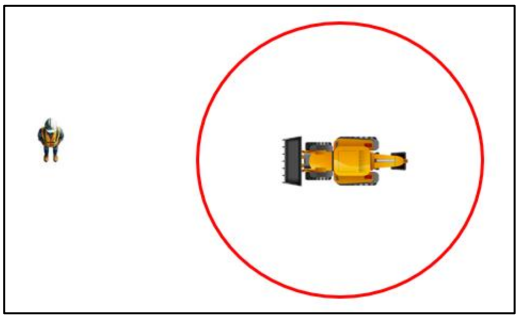

(b)

Figure 4. Model evaluation strategy (a) Proposed hazard zone (b) Static circular hazard zone

A total of 100 simulations were conducted for both hazard zones, with varying worker locations and equipment speeds. The worker's location was randomly varied both in the longitudinal and cross-sectional directions. To keep the location within a reasonable range, the location is kept within a 30 m range across the road, i.e. 15 m from the centerline of the equipment in both directions, and 100 m range along the road. The equipment speed was sampled from a normal distribution with a mean of 10 kph and a standard deviation of 5 kph. To ensure realistic speeds for construction equipment, the minimum and maximum speed values were set at 5 kph and 20 kph, respectively.

The proposed model has variables including equipment footprint, initial safety boundary, the speed of equipment, and deceleration rate of the equipment. These variables were set before running the simulation, except for the speed of equipment which is variable. The equipment footprint was directly measured for the specific equipment used in the simulation to be 3 meters long and 1.7 meters wide. The initial safety boundary is taken to be 2 meters as is recommended by Shen et al. [5] and Wang et al. [6]. The deceleration rate, which is the rate at which the equipment decreases its speed when the brake is applied, was obtained to be 1.05 m/s^2 for the specific equipment used in the simulation.

3.3 Evaluation Criteria

After completing the necessary setup, the simulation was then run, and results were categorized into true positives, true negatives, false positives, and false negatives, with the following meanings:

- **False Negative (FN):** The equipment hits or dangerously approaches the worker, indicating a failure to alert in time. This indicates that the model couldn't timely recognize a positive case and gave a false safety, leading to a dangerous situation. A trial is classified as false negative if the equipment hits the worker or the worker comes within a 1-meter distance around the equipment footprint at any time during the equipment's movement or when the equipment finally stops.
- **False Positive (FP):** The equipment stops too far from the worker or passes safely, yet the system triggers an unnecessary alert. Previous literature provides little guidance on the appropriate distance between the worker and equipment to classify it as "too far". In a field experiment by Teizer et al. [7], equipment stopping at least 10 meters away from the worker was considered safe. This value is adopted as the criterion in this study to differentiate false positives from true positives, along the direction of equipment movement. However, applying the 10-meter threshold to the width of the equipment is deemed unreasonable, as it would be overly conservative and result in many false alarms being classified as true positives. Therefore, the width threshold is set at one standard lane width, i.e., 3.6 meters, from the equipment. Accordingly, a false positive occurs when the equipment stops while the worker is outside the 10 meters by 3.6 meters boundary.
- **True Positive (TP):** The equipment stops safely with the worker at a safe distance, indicating that the system correctly detected the danger.
- **True Negative (TN):** The worker is located at a safe distance from the equipment and no alert is issued, as expected.

4 Results and Discussion

Following the methodology described, a total of 100 simulations were conducted for both the proposed dynamic hazard zone model and a conventional static circular hazard zone. The simulations accounted for varying worker locations and equipment speeds, ensuring diverse scenarios for evaluation. The simulation results showed that the proposed hazard zone model classified 93% of trials correctly while the static circular hazard zone correctly classified 60% of trials. The total number of cases classified as true positives, true negatives, false positives, and false negatives are presented in Figure 5.

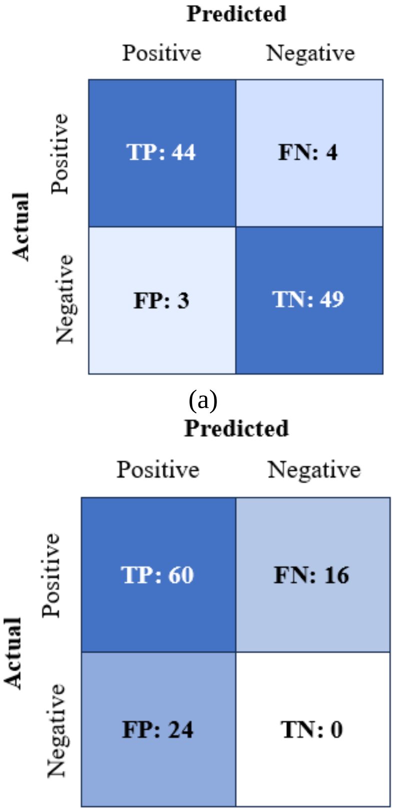

(b)

Figure 5. Confusion matrix (a) Proposed hazard zone (b) Static circular hazard zone

It can be clearly seen that the circular hazard zone struggled to identify negative cases and classified them as false positives. In addition, the static circular hazard zone was less efficient in detecting true positive cases, as it classified more cases as false negatives than the proposed hazard zone. This occurred because the static circular hazard zone used a fixed radius for varying equipment speed values, leading to false negatives at higher speeds and false positives at lower speeds. To further understand the performance of the proposed dynamic hazard zone model, the results were analyzed based on different speed ranges of construction equipment. The findings are summarized in Table 1.

Table 1. Breakdown of model performance across

different speed ranges

Speed Range	Hazard Zone	TP	TN	FP	FN	ACC
5–10 kph	Proposed	20	22	1	1	95.5%
	Static	37	0	12	0	75.5%
10–15 kph	Proposed	19	20	1	2	92.9%
	Static	17	0	9	12	44.7%
15–20 kph	Proposed	5	7	1	1	85.7%
	Static	6	0	3	4	46.2%

The results highlight the following key points:

- **Low Speeds (5–10 kph):** The proposed model demonstrated high accuracy (95.5%) with minimal false positives (1) and false negatives (1), effectively distinguishing between hazardous and safe scenarios. In comparison, the static model achieved lower accuracy (75.5%) due to a higher number of false positives (12).
- **Medium Speeds (11–15 kph):** At medium speeds, the proposed model maintained strong performance with an accuracy of 92.9%. The static model, however, exhibited significant performance degradation, with an accuracy of only 44.7% due to large number of false positives (9) and false negatives (12). This decline in performance is primarily because, despite the increase in speed, the static hazard zone remains unchanged, treating equipment moving at higher speeds the same as slower-moving equipment. As a result, the static model fails to account for the increased stopping distance and reaction time, leading to false negatives, where a real hazard is incorrectly classified as non-hazardous. This limitation highlights the advantage of the proposed model, which dynamically adjusts the hazard zone based on speed variations, ensuring more accurate hazard identification.
- **High Speeds (16–20 kph):** The proposed model achieved an accuracy of 85.7%, with a slight decrease compared to lower speeds. This indicates that the model still remains effective even at higher speeds. In contrast, the static model struggled significantly, achieving only 46.2% accuracy. These results reinforce the adaptability of the proposed model compared to static hazard zones.

While the simulation results demonstrate the proposed model's effectiveness, its validation in a controlled virtual environment limits generalizability to real-world conditions, where factors like unpredictable worker behavior, sensor inaccuracies, and environmental variables may influence performance. To address these challenges, field testing is essential to assess the model's accuracy and robustness under diverse, dynamic scenarios involving varying equipment types and operational conditions.

5 Limitations

While the proposed probabilistic hazard zoning model performs well in the simulated environment used in this study, several real-world challenges may affect its practical implementation. Real-world sensors are subject to noise and drift, which can introduce inaccuracies in position tracking and cause deviations in hazard zone boundaries. To mitigate this, effective sensor fusion techniques should be employed to enhance location reliability. Additionally, in highly dynamic environments such as highway work zones, unpredictable worker behavior and complex interactions between workers and construction equipment present further challenges. Adapting the proposed model for such scenarios will require future work focused on incorporating predictive techniques for worker movement patterns and worker-equipment interactions. Field validation through real-world deployments will also be essential to refine the model and optimize its parameters for practical applications.

6 Conclusion

This study developed a dynamic hazard zone model to address the limitations of traditional static circular hazard zones in highway work zones. By employing a probabilistic approach using a bivariate Gaussian distribution, the proposed model generates adaptive hazard zones that account for real-time changes in equipment speed and movement. The proposed model's effectiveness was validated through simulations, where it demonstrated superior performance compared to static circular hazard zones, achieving 93% accuracy in correctly classifying hazard scenarios. The findings highlight the significant potential of dynamic hazard zones in enhancing worker safety by accurately detecting true hazards and minimizing false alarms, even in highly dynamic environments. This approach not only reduces the risk of near-miss incidents and collisions but also minimizes disruptions caused by unnecessary alerts. Future work could focus on validation through field experiments and refinement of the model for more accuracy.

Acknowledgements

The authors would like to acknowledge the funding (Grant No. 1036338) provided by the Minnesota Department of Transportation (MNDOT) to conduct this study.

References

[1] M. Osman, R. Paleti, and S. Mishra, “Analysis of passenger-car crash injury severity in different work zone configurations,” *Accid Anal Prev*, vol. 111, pp. 161–172, Feb. 2018, doi: 10.1016/J.AAP.2017.11.026.

[2] N. S. S. Al-Bdairi, “Does time of day matter at highway work zone crashes?,” *J Safety Res*, vol. 73, pp. 47–56, Jun. 2020, doi: 10.1016/J.JSR.2020.02.013.

[3] J. M. Wong, M. C. Arico, and B. Ravani, “Factors influencing injury severity to highway workers in work zone intrusion accidents,” *Traffic Inj Prev*, vol. 12, no. 1, pp. 31–38, Feb. 2011, doi: 10.1080/15389588.2010.525569.

[4] K. Elelu, T. Le, and C. Le, “Collision Hazard Detection for Construction Worker Safety Using Audio Surveillance,” *J Constr Eng Manag*, vol. 149, no. 1, p. 04022159, Nov. 2022, doi: 10.1061/JCEMD4.COENG-12561.

[5] X. Shen, E. Marks, N. Pradhananga, and T. Cheng, “Hazardous Proximity Zone Design for Heavy Construction Excavation Equipment,” *J Constr Eng Manag*, vol. 142, no. 6, p. 05016001, Jan. 2016, doi: 10.1061/(ASCE)CO.1943-7862.0001108.

[6] J. Wang and S. N. Razavi, “Low False Alarm Rate Model for Unsafe-Proximity Detection in Construction,” *Journal of Computing in Civil Engineering*, vol. 30, no. 2, Mar. 2016, doi: 10.1061/(asce)cp.1943-5487.0000470.

[7] J. Teizer, B. S. Allread, C. E. Fullerton, and J. Hinze, “Autonomous pro-active real-time construction worker and equipment operator proximity safety alert system,” *Autom Constr*, vol. 19, no. 5, pp. 630–640, Aug. 2010, doi: 10.1016/j.autcon.2010.02.009.

[8] J. W. Park, X. Yang, Y. K. Cho, and J. Seo, “Improving dynamic proximity sensing and processing for smart work-zone safety,” *Autom Constr*, vol. 84, pp. 111–120, Dec. 2017, doi: 10.1016/J.AUTCON.2017.08.025.

[9] I. Abotaleb, K. Nassar, and O. Hosny, “Layout optimization of construction site facilities with dynamic freeform geometric representations,” *Autom Constr*, vol. 66, pp. 15–28, Jun. 2016, doi: 10.1016/J.AUTCON.2016.02.007.

[10] J. Wang and S. Razavi, “Two 4D Models Effective in Reducing False Alarms for Struck-by-Equipment Hazard Prevention,” *Journal of Computing in Civil Engineering*, vol. 30, no. 6, p. 04016031, Nov. 2016, doi: 10.1061/(ASCE)CP.1943-5487.0000589/ASSET/194B8CA0-62E0-4FA5-99AB-0273D5464CAF/ASSETS/IMAGES/LARGE/FIGURE12.JPG.

[11] J. Teizer and T. Cheng, “Proximity hazard indicator for workers-on-foot near miss interactions with construction equipment and geo-referenced hazard areas,” *Autom Constr*, vol. 60, pp. 58–73, Dec. 2015, doi: 10.1016/j.autcon.2015.09.003.

[12] I. G. Awolusi, E. D. Marks, N. Pradhananga, and T. Cheng, “Hazardous proximity zone design for heavy construction equipment,” 2015, doi: 10.14288/1.0076403.

[13] I. Awolusi and E. D. Marks, “Active work zone safety: Preventing accidents using intrusion sensing technologies,” *Front Built Environ*, vol. 5, p. 431578, Mar. 2019, doi: 10.3389/FBUIL.2019.00021/BIBTEX.

[14] B. W. Jo, Y. S. Lee, J. H. Kim, D. K. Kim, and P. H. Choi, “Proximity Warning and Excavator Control System for Prevention of Collision Accidents,” *Sustainability 2017, Vol. 9, Page 1488*, vol. 9, no. 8, p. 1488, Aug. 2017, doi: 10.3390/SU9081488.

[15] X. Luo, H. Li, T. Huang, and T. Rose, “A field experiment of workers’ responses to proximity warnings of static safety hazards on construction sites,” *Saf Sci*, vol. 84, pp. 216–224, Apr. 2016, doi: 10.1016/J.SSCI.2015.12.026.

[16] J. Teizer, “Magnetic Field Proximity Detection and Alert Technology for Safe Heavy Construction Equipment Operation,” 2015.

[17] J. Park, Y. K. Cho, and A. Khodabandelu, “Sensor-Based Safety Performance Assessment of Individual Construction Workers,” *Sensors 2018, Vol. 18, Page 3897*, vol. 18, no. 11, p. 3897, Nov. 2018, doi: 10.3390/S18113897.

[18] Z. Zhang, W. Li, and J. Yang, “Analysis of stochastic process to model safety risk in construction industry,” *Journal of Civil Engineering and Management*, vol. 27, no. 2, pp. 87–99, Feb. 2021, doi: 10.3846/JCEM.2021.14108.

[19] K. N. Abdrakhmanova, A. V. Fedosov, K. R. Idrisova, N. K. Abdrakhmanov, and R. R. Valeeva, “Review of modern software complexes and digital twin concept for forecasting emergency situations in oil and gas industry,” *IOP Conf Ser Mater Sci Eng*, vol. 862, no. 3, p. 032078, May 2020, doi: 10.1088/1757-899X/862/3/032078.

[20] W. Umer and M. K. Siddiqui, “Use of Ultra Wide Band Real-Time Location System on Construction Jobsites: Feasibility Study and Deployment Alternatives,” *Int J Environ Res*

Public Health, vol. 17, no. 7, Apr. 2020, doi: 10.3390/IJERPH17072219.

[21] A. Y. Demeke *et al.*, "Advancing Highway Work Zone Safety: A Comprehensive Review of Sensor Technologies for Intrusion and Proximity Hazards," *https://doi.org/10.1177/03611981241265845*, Aug. 2024, doi: 10.1177/03611981241265845.

[22] N. Soltanmohammadlou, S. Sadeghi, C. K. H. Hon, and F. Mokhtarpour-Khanghah, "Real-time locating systems and safety in construction sites: A literature review," *Saf Sci*, vol. 117, pp. 229–242, Aug. 2019, doi: 10.1016/J.SSCI.2019.04.025.

[23] M. Younesi Heravi, I. S. Dola, Y. Jang, and I. Jeong, "Edge AI-Enabled Road Fixture Monitoring System," *Buildings 2024, Vol. 14, Page 1220*, vol. 14, no. 5, p. 1220, Apr. 2024, doi: 10.3390/BUILDINGS14051220.

[24] I. Jeong, Y. Jang, I. Sharmin Dola, and M. Younesi Heravi, "A Framework for Remote Road Furniture Monitoring System Using Smart IoT Dashcams and Digital Twin," *Computing in Civil Engineering*, pp. 1080–1088, 2024, doi: 10.1061/9780784485248.129.

[25] H. Kim and S. Han, "Accuracy Improvement of Real-Time Location Tracking for Construction Workers," *Sustainability 2018, Vol. 10, Page 1488*, vol. 10, no. 5, p. 1488, May 2018, doi: 10.3390/SU10051488.

[26] J. Teizer *et al.*, "Construction resource efficiency improvement by Long Range Wide Area Network tracking and monitoring," *Autom Constr*, vol. 116, p. 103245, Aug. 2020, doi: 10.1016/J.AUTCON.2020.103245.

[27] MUTCD, "Chapter 2C - MUTCD 2009 Edition - FHWA." Accessed: Jun. 03, 2024. [Online]. Available: https://mutcd.fhwa.dot.gov/htm/2009/part2/part2c.htm

[28] "Cyberbotics: Robotics simulation with Webots." Accessed: Oct. 21, 2024. [Online]. Available: https://cyberbotics.com/#webots